As originally published in the IPC APEX EXPO Proceedings.

Reliability and Microstructure of Lead-Free Solder Joints in Industrial Electronics after Accelerated Thermal Aging

Francesca Scaltro[†], Mohammad H. Biglari[†§], Alexander Kodentsov[‡], Olga Yakovleva[†], Erik Brom[†]
[†]Mat Tech BV, Son, The Netherlands; [‡]Department of Materials and Interface Chemistry, University of Technology of Eindhoven, The Netherlands;
[§]corresponding author: m.biglari@mat-tech.com, telephone +31 499 490133

Abstract
The reliability of lead-free (LF) solder joints in surface-mounted device components (SMD) has been investigated after thermo-cycle testing. Kirkendall voids have been observed at the interface component/solder together with the formation of fractures. The evolution, the morphology and the elemental analysis of the intermetallic layer have been evaluated before and after the thermal treatment.

Voids produced by the release of volatile species during the soldering process due to the application of flux were present. If compared with SnPb soldered systems, lead-free joints are characterized by larger and a higher amount of voids. In several electronic joints (ball grid arrays (BGA), surface-mounted device components (SMD), etc.) fractures developed after the thermal stresses generated during the accelerated thermal aging. Warpage of the PCB has also been observed. Backward and forward compatibility of SnPb and lead-free BGA connections has been performed on pads with an ENIG finish. The effect of the reflow peak temperature on the structure of the intermetallic layer has been assessed.

1 Introduction

Lead containing alloys have maintained for their characteristics (i.e. low cost, low surface tension, low eutectic temperature, high strength, high heat dissipation, etc.) a predominant role in soldering alloy compositions for many decades.[1] However, the use of lead in consumer electronics has been restricted by RoHS since July 1st 2006 because of its high toxicity.[2] Therefore lead, among other materials, had to be replaced with more environmental friendly and less toxic substances. Among the potential candidates for the replacement of lead in conventional SnPb solders, alloys based on Sn, Ag and Cu (SAC) near the eutectic composition are regarded as the most promising because of their high wettability and relatively low eutectic temperature (217°C).[3-4] Nevertheless, the properties of lead-free alloys do not often satisfy the requirements of long time mechanical and chemical stability and several issues regarding the failure mechanisms and service life prediction must find elucidation.

The reliability of a joint depends on the physical, mechanical and chemical properties of the intermetallic layer. The intermetallic layer (IMC) is a dynamic interface which evolution depends on several factors: the composition of the materials joint together, the thickness of the different components, the temperature used during the reflow process and the temperature that the intermetallic layer has to outstand during the service life conditions of the component.

Electroless nickel immersion gold (ENIG) finishes are a known example of potential brittle fracture of a soldered joint during service life conditions. Phosphorous is generally used to protect the nickel finish from corrosion during the application of a gold layer by acidic immersion. It is documented that phosphorous has the tendency, during soldering, to create a phosphorous-rich phase at the interface between the solder and the layer of Ni(P). The growth of this intermetallic layer during service life conditions can lead to the he phenomena known as "black pad" and/or to "mud-cracking" at the interface between the intermetallic layer and the Ni(P) layer. Those effects lead to an inevitable failure of the joint and to the need of replacement of the component.

Additional reliability concerns rise from the forced combination of lead-free and lead- containing alloys and/or metallurgical processes. In fact, because of the investments in lead-free industry, the availability of all components present in an assembly, made with the conventional lead-containing material, is not feasible any longer. Therefore, most times mixtures of lead-containing and lead-free materials are present in assembled materials.

In this study the effects of mixing lead-containing (SnPb) and lead-free (SAC) soldering technology on the microstructure of the intermetallic layer (IMC) are described. In addition, the evolution of the intermetallic layer after accelerated thermal aging is evaluated.

2 Experimental

2.1 Materials

SnPb-BGAs soldered with SnPb paste (paragraph 3.1) or LF-paste (paragraph 3.2) were investigated. For all BGAs, the PCB surface had an ENIG finish of comparable thickness; the gold finish was of approximately 0.03 μm. The composition of the component alloy was 64 wt% Sn, 36 wt% Pb. No-clean flux was used. The reflow peak temperature used during the soldering process is generally 20-40°C above the melting temperature of the employed solder alloy. Therefore the peak temperature reached for SnPb alloys is about 208-225°C while the reflow peak temperature reached for lead-free alloys is about 235-250°C. In this study, the effect of mixing metallurgical processes has been investigated. SnPb-BGA with SnPb paste was soldered using a conventional lead-free profile process with a peak temperature of 235°C. SnPb-BGA with LF-paste was soldered using a conventional lead-containing profile process with a peak temperature of 225°C. Samples were analyzed by means of optical microscopy, SEM and EDX analysis.

LF-BGAs soldered with SnPb paste were investigated. For all BGAs, the PCB surface had an ENIG finish of comparable thickness. The composition of the component alloy was SAC305. No-clean flux was used. The effect of mixing different metallurgical processes has been investigated. LF-BGA with SnPb-paste was soldered using conventional lead-free profile process with a peak temperature of 235°C (paragraph 3.3) or conventional lead-containing profile process with a peak temperature of 225°C (paragraph 3.4). Samples were studied by means of optical microscopy, SEM and EDX analysis.

LF-Quad Flat Pack components (QFP) soldered with LF-paste have been investigated before and after thermal cycle tests (paragraphs 3.5 and 3.6). All copper pads on the PCB surface had an ENIG finish. SAC305 paste and no-clean flux were used for soldering. A typical lead-free reflow process in air was applied. Several samples of similar compositions have been investigated. Only the most representative images are described. In order to understand reliability issues, improve the solder stability and/or predict the reliability of lead free joints, it is necessary to know and understand the structural changes, as a function of time, that are taking place at the interface during service life conditions. For this purpose, accelerated solid state thermal aging was performed: the sample is subject to temperature cycles and the reliability is tested in a reasonable short time scale. The testing temperature ranged from -40ºC to +125ºC; the heating and cooling step was done at 2.75ºC/min. Each cycle was carried out with 20 minutes of dwell time at the extreme temperatures (-40°C and +125°C). The total testing process consisted of 1256 cycles. Samples were analyzed by means of optical microscopy, SEM and EDX.

2.2 Characterization techniques

The samples that had to be analyzed were cut from the original matrix. In order to investigate the microstructure of the interfaces, a cross section of the samples was prepared by embedding the sample in a conductive material (Technovit 5000). After hardening of the embedding material (approximately one hour in N_2 atmosphere), the samples were first coarsely grinded with sandpaper and finally polished with a diamond suspension (1/4 micrometer particles). When the desired smoothness of the surface was reached, the samples were rinsed with distillated water and sonicated for a few minutes in alcohol in order to remove loose particles and residues of the material used during the preparation stages.

Microstructure changes have been evaluated by optical and scanning electron microscopy together with EDX analysis. All light optical microscopy investigations were carried on with an Olympus BX-41 microscope while scanning electron images (SEM) and EDX analysis were performed on a Jeol JSM-5600. The voltage used, for the SEM and the EDX analysis, was, if not specifically indicated, 15 KeV.

3 Results and Discussion

3.1 SnPb-BGA and SnPb-paste: backward and forward compatibility (T_{peak} = 235°C)

Two different magnifications of a cross section of SnPb-BGA soldered with SnPb-paste are present in Figure 1. The illustrated portion is the interface SnPb-BGA/pad. The SnPb-BGA was soldered using a standard lead-free reflow soldering profile with a peak temperature of 235°C.

The SnPb alloy shows the typical morphology of those alloys. The Sn-Ni intermetallic layer (Ni_3Sn_4) is approximately five micrometers thick. Micrometer (Kirkendall) voids are visible both at the interface SnPb-BGA/IMC and at the interface Ni/Cu.

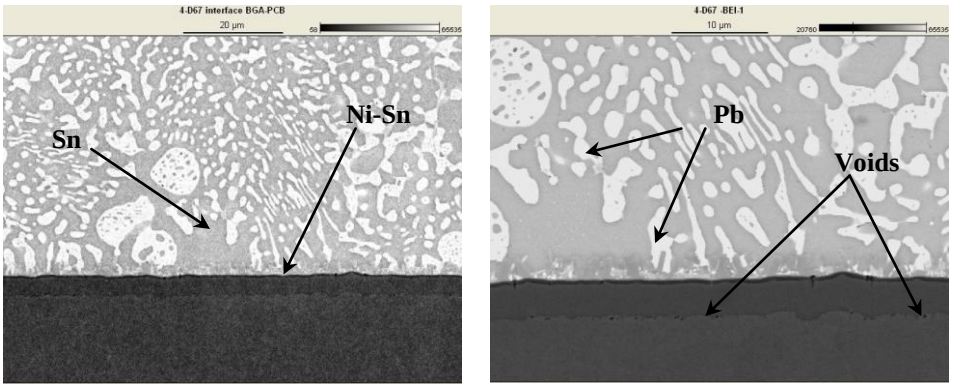

Figure 1 - Cross section of a SnPb-BGA soldered with SnPb-paste; (a) and (b) different magnification images of a sample prepared with a reflow peak temperature of 235°C (secondary electron images).

3.2 SnPb-BGA and LF-paste: failure analysis (T_{peak} = 225°C)

The cross section of a SnPb-BGA soldered with LF-paste without apparent defects is shown in Figure 2a.

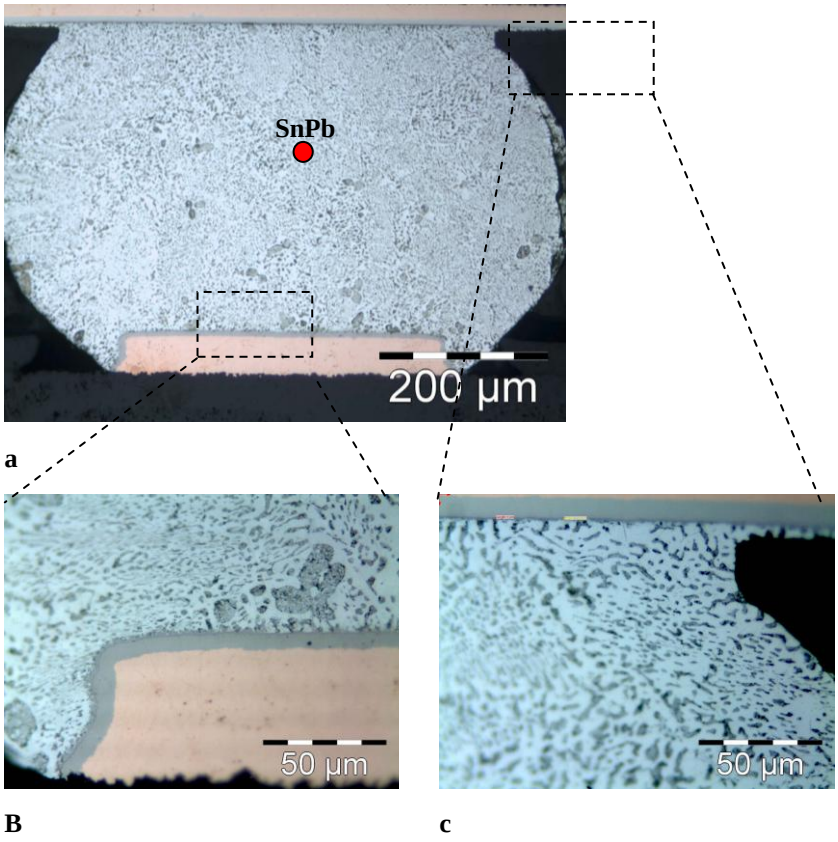

Figure 2 - (a) Cross section of a good quality SnPb-BGA soldered with LF-paste; (b) enlargement of the intermetallic layer at the interface SnPb-BGA/pad; (c) enlargement of the intermetallic layer at the interface component/SnPb-BGA (optical microscope images). EDX analysis was performed on the area highlighted by the red dot in Figure 2a.

The enlargements of a portion of the intermetallic layer at the component side and at the PCB side are presented as well (Figures 2b and 2c). All samples shown in this section were soldered using a standard lead-containing reflow soldering profile with a peak temperature of 225°C.

The morphology of the BGA is typical of SnPb alloys. From EDX analysis, the composition of the BGA resulted being 14 wt% of Sn and 86 wt% of Pb (EDX was performed on the red spot area present in Figure 2a). The lead phase is homogeneously distributed all over the BGA section. This is an essential feature for the reliability of BGAs under thermal fatigue. It is in fact known that an incomplete amalgamation of the components may lead to an early failure of the mixed solder joints. The distribution of the Pb all over the area depends on the reflow procedure and on the peak temperature applied. The thickness of the intermetallic layer on the as-reflowed samples was evaluated to be, from secondary electronic images evaluation, of 1-1.10 micrometers at the component side and of 1.61 - 3.21 micrometers on the PCB side.

The copper pad substrate had an ENIG metallization; in fact, phosphorous was detected from the EDX analysis (Figures 3a and 3b). The EDX analysis indicated the presence of 11.67 at% of P and 88.33 at% of Ni.

The Ni-layer on the component side was instead a galvanic layer; as such, no phosphorous was detected by EDX analysis (Figures 3c and 3d).

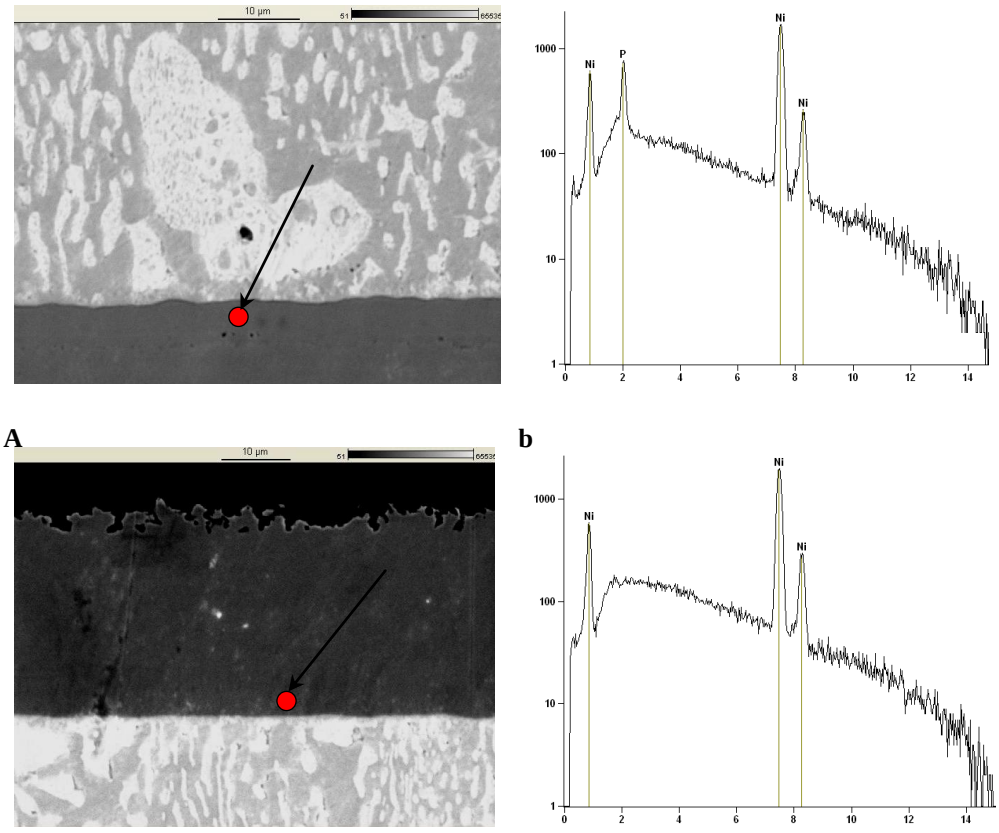

Figure 3 - SEM cross section enlargement and correspondent EDX analysis of the Ni finish from (a)-(b) the pad side and (b)-(d) from the component side in SnPb-BGA soldered with LF-paste. The EDX analysis was performed on the area highlighted by the red dot on the respective images.

Rarely, at the interface SnPb-BGA/intermetallic layer, an intermetallic gold phase (Au-Sn-Ni) was found.

In all cases, no fractures were observed at the component side. A portion of the interface at the component side for two different samples is shown, as an example, in Figures 4a and 4b.

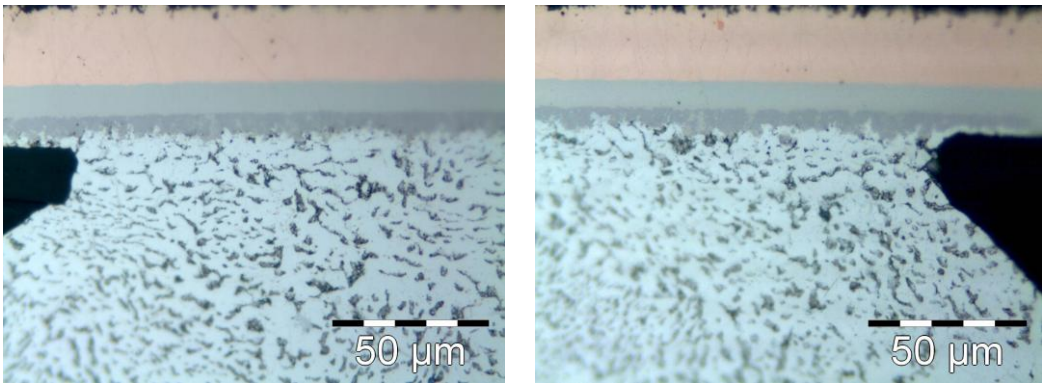

a b

Figure 4 - (a) and (b) typical cross sections of different SnPb-BGAs soldered with LF-paste at the interface component/SnPb-BGA (optical microscope images).

In Figure 5 typical cross sections of BGAs with visible defects are shown. Occasionally, voids due to residues of flux are present (Figure 5a). Among all the samples investigated (76 in total) around 50% of them developed fractures, after the reflow process, at the pad side. The most common failure of those components was due to the developing of a fracture (partial or total) at the intermetallic layer. Warpage and shift of the SnPb-BGAs from the initial location (Figures 5b, 5c and 5d) have been observed as well.

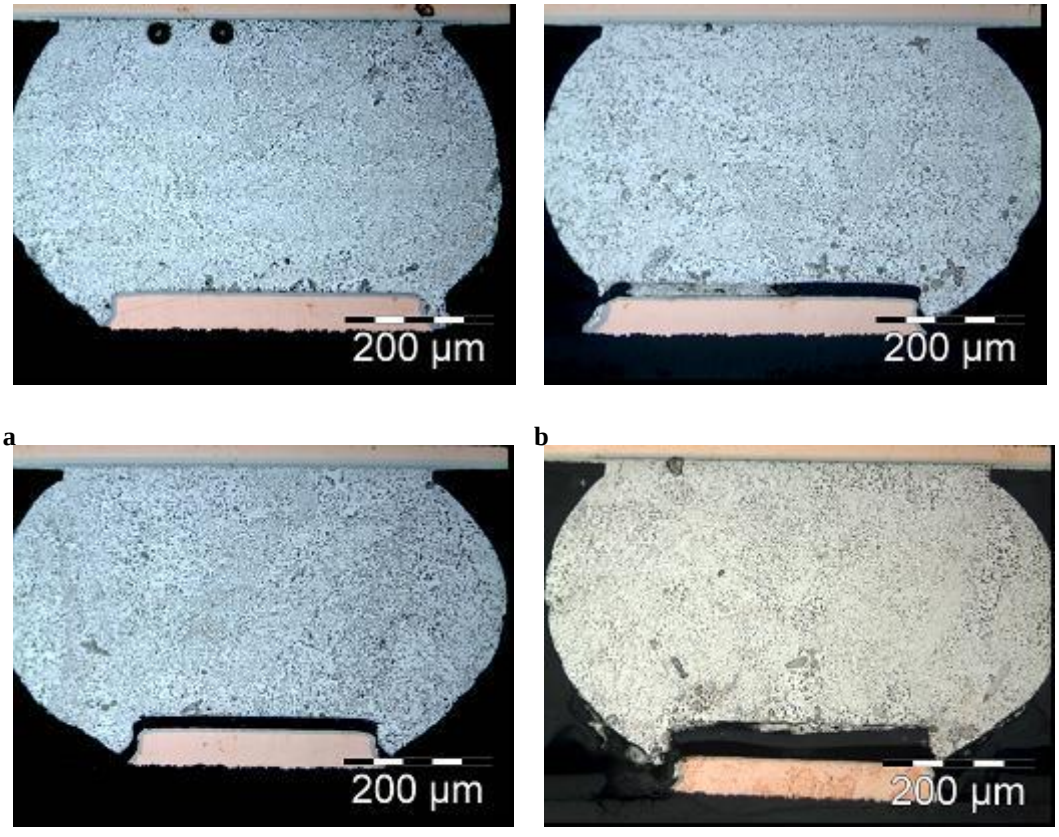

a b

c d

Figure 5 - Cross sections of defected as-reflowed SnPb-BGAs soldered with LF-paste, (optical microscope images): (a) voids due to flux residues; (b) fracture at the BGA/Ni interface with residual material at the interface and (c) without any material at the interface; (d) fracture and shift of the BGA from the initial position.

In some cases, fractures were found at the interface pad/PCB as illustrated in Figures 6a and 6b.

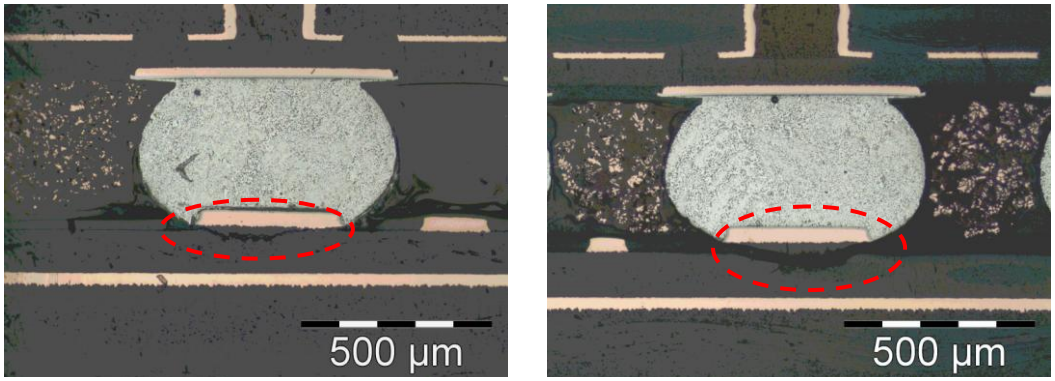

A **b**

Figure 6 - Cross sections of fractured as-reflowed SnPb-BGAs soldered with LF-paste (optical microscope images).

From the EDX analysis it was revealed that in many of the fractured joints (approximately half of the ones that presented a failure) another phase is present in the fracture. In Figure 7, an optical microscope image, a secondary electron image and the elemental analysis on two different areas, indicated by the red and the white dot, of such phase are presented. The main components of this material are Sn, Pb and Ni.

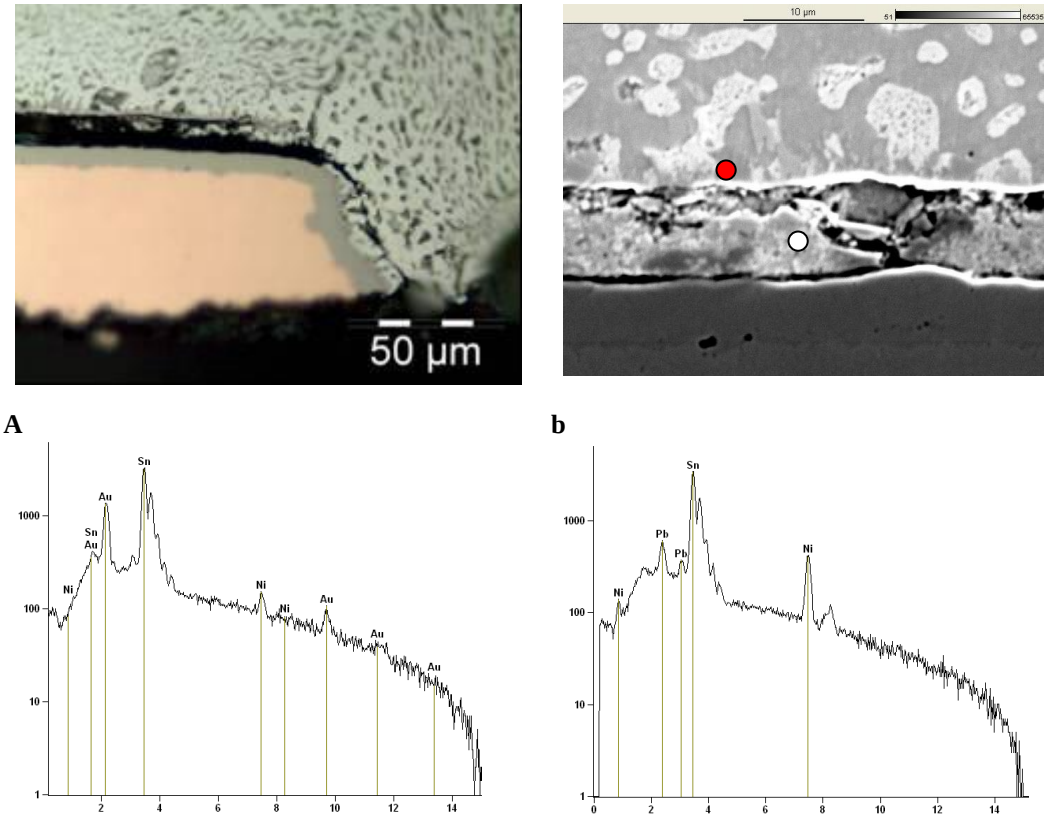

A **b**

c (red dot) **d (white dot)**

Figure 7 - (a) Optical microscope image and (b) secondary electron image of a cross section of a fractured SnPb-BGA soldered with LF-paste, enlargement. (c) and (d), EDX signal of the area highlighted respectively with a red and white dot in Figure 7b.

In Figure 8 the microstructure analysis of another fractured SnPb-BGA is presented.

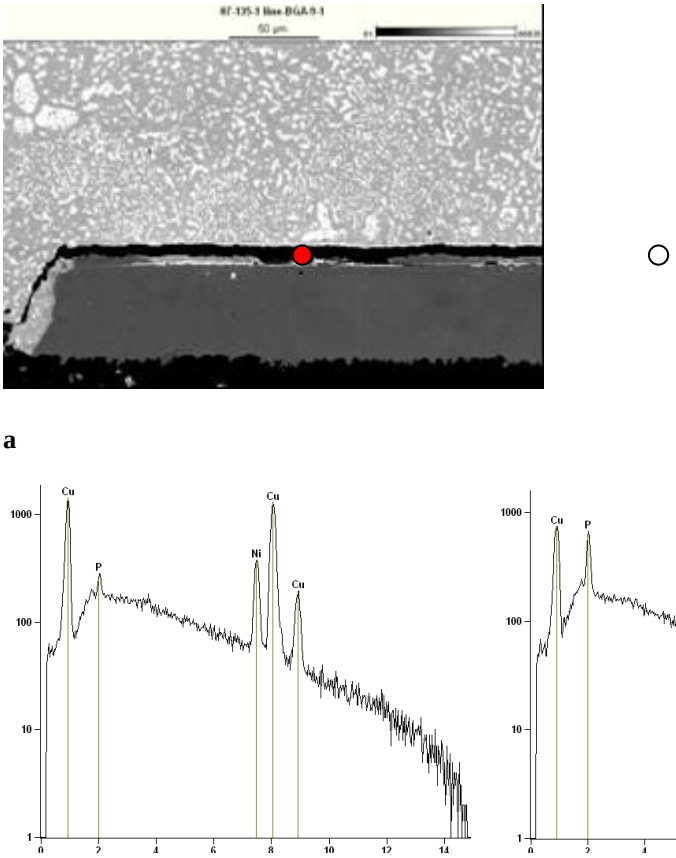

Figure 8 - (a) Secondary electron image of a fracture of a SnPb-BGA soldered with LF-paste; (b) and (c) EDX signal of the areas at the top side of the fracture on the pad side highlighted by the red and white dot in Figure 8a.

The composition in the position highlighted with the red and white dot are respectively of 1.77 at% P, 16.81 at% Ni, 81.42 at% Cu and 8.18 at% P, 56.95 at % Ni, 34.87 at% Cu.

The fracture is in all cases irregular. It is know that the presence of phosphorous can affect greatly the reliability of joints. A thick phosphorous enriched nickel layer is a potential of brittle fracture.

In some areas, gold intermetallic layers containing gold (Au-Sn-Ni) were observed by elementals analysis (Figures 7c and 9).

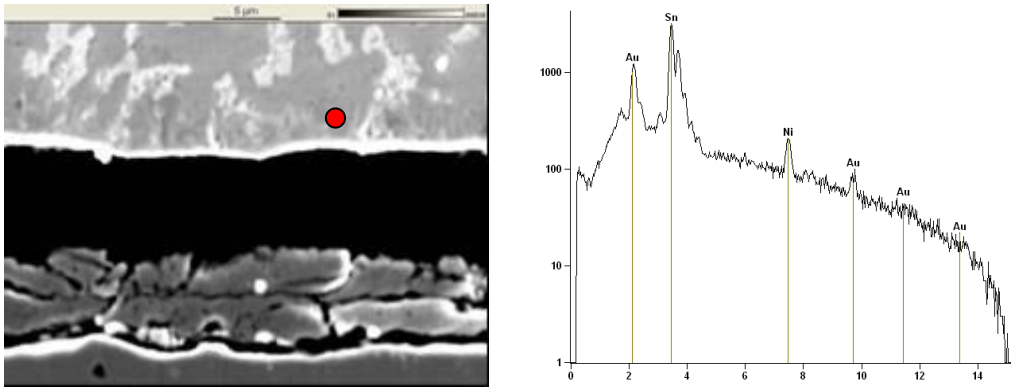

Figure 9 - (a) Cross section of a fractured SnPb-BGA soldered with LF-paste (secondary electron image); portion of the interface at the pad side; (b) EDX signal of the area highlighted with the red sphere in Figure 9a.

3.3 LF-BGA and SnPb-paste: backward and forward compatibility (T_{peak} = 235°C)

The cross section of a LF-BGA and SnPb-paste soldered with a reflow peak temperature of 235°C is shown in Figure 10.

The as-reflowed BGA ball is composed of a Sn matrix, Ag_3Sn and Sn-Cu-Ni intermetallics. The lead phase, from the SnPb-paste, forms coarse particle distributed all over the BGA cross section. In addition, globular shaped phases consisting of Sn-Ni-Cu are observed. Those phases might be generating because of defects in the Ni barrier. Although those phases developed across the joint interface, no marked Sn-Cu-Ni intermetallic layer was found between the solder and the ENIG finish.

Also in this case, micrometer voids (Kirkendall voids) due to the unbalanced diffusion of the atoms present at the interfaces are present both at the SnPb/IMC and Ni/Cu interfaces.

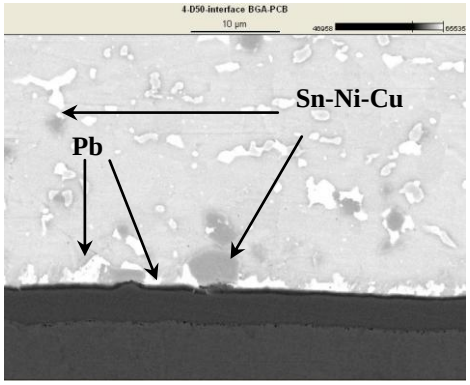

Figure 10 - Cross section of a LF-BGA soldered with SnPb-paste; the sample was prepared with a reflow peak temperature of 235°C (secondary electron images).

3.4 LF-BGA and SnPb-paste: backward and forward compatibility (T_{peak} = 225°C)

A portion of the cross section of a LF-BGA soldered with SnPb-paste using a standard lead-containing solder profile, i.e. a reflow process with a peak temperature of 225°C, is shown in Figure 11.

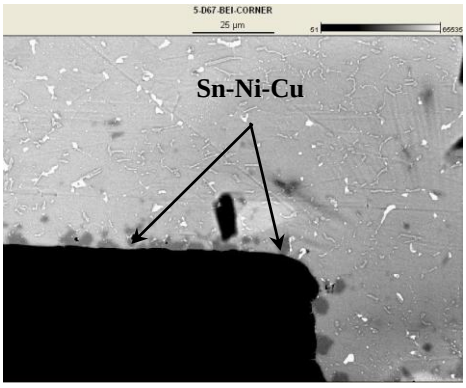

Figure 11 - Cross section of a LF-BGA soldered with SnPb-paste; the sample was prepared with a reflow peak temperature of 225°C (secondary electron images).

The lead phase morphology in lead-free solders does not significantly change by using a reflow peak temperature of 225°C instead of 235°C (the latter was described in the previous paragraph). The Sn-Ni-Cu phase particles appear located more closely to the pad interface (Figure 11) if compared when using a peak temperature of 235°C (Figure 10). In Figure 12 the secondary electron images of a LF-BGA soldered with SnPb-paste with a peak temperature of 225°C are shown. It is evident that the presence of Pb in mixed solders, no matter the peak temperature used, inhibits the formation of a thick intermetallic layer by obstructing the diffusion of copper towards the joint. In addition, the formation of the intermetallic particles (Sn-Ni-Cu) seems to have origin were the lead barrier (white phase in the secondary electron images) is not visible. The Pb at the interface of the LF-BGA intermetallic layer is generated by segregation of the lead phase. At the interface, during the soldering interface, Ni reacts with Sn to form Ni_3Sn_4, consuming the Sn locally present. Due to the faster diffusion of Sn, if compared to Pb, a higher concentration of Pb will be present locally and segregation therefore occurs.

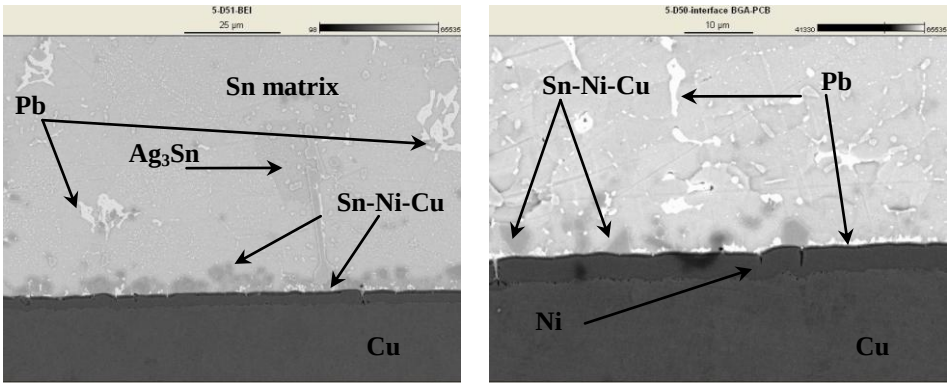

A **b**

Figure 12 - Cross section of a LF-BGA soldered with SnPb solder paste, the sample was prepared by a reflow peak temperature of 225°C (secondary electron images).

3.5 LF-QFP and LF-paste: before accelerated thermal cycling test

A portion of the cross section of an as-reflowed quad flat component (QFP) is present in Figure 13: no large defects or fractures are visible after reflowing.

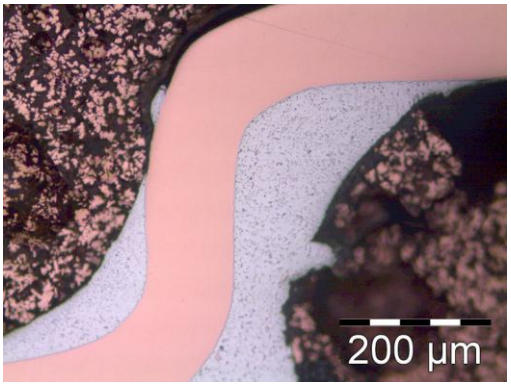

Figure 13 - Cross section of an as-reflowed LF-component soldered using LF-paste (optical microscope image).

During the reflow process the gold layer on the ENIG finish melts thus Ni has the ability to react with Sn and Cu, forming intermetallics. The intermetallic layer thickness, evaluated from secondary electron images, is about two micrometers.

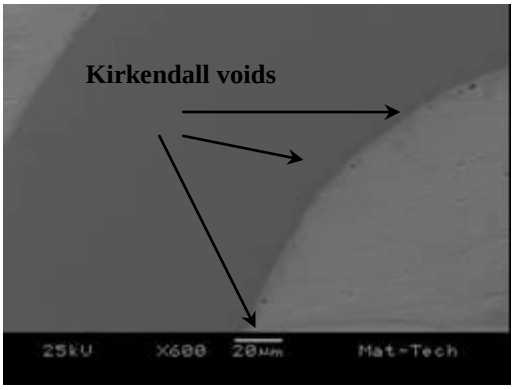

Figure 14 - Cross section of an as-reflowed LF-component soldered using LF-paste. Kirkendall voids at the component/LF paste interface are indicated (secondary electron image).

Kirkendall voids are observed at the interface component/LF-paste (Figure 14) and at the interface LF-paste/PCB component. Those voids are caused by the different diffusion rate of Sn and Cu atoms. After being generated, the small gaps coalesce and form visible micrometer holes.

In Figure 15 some details of LF-components of different QFPs are shown. The often present large voids are caused by the interaction of flux and the lower density of LF-alloys.

In general, larger and more voids were observed for the LF alloys in comparison to the Sn-Pb alloys. The presence of such large defects might dangerously affect the reliability of the component.

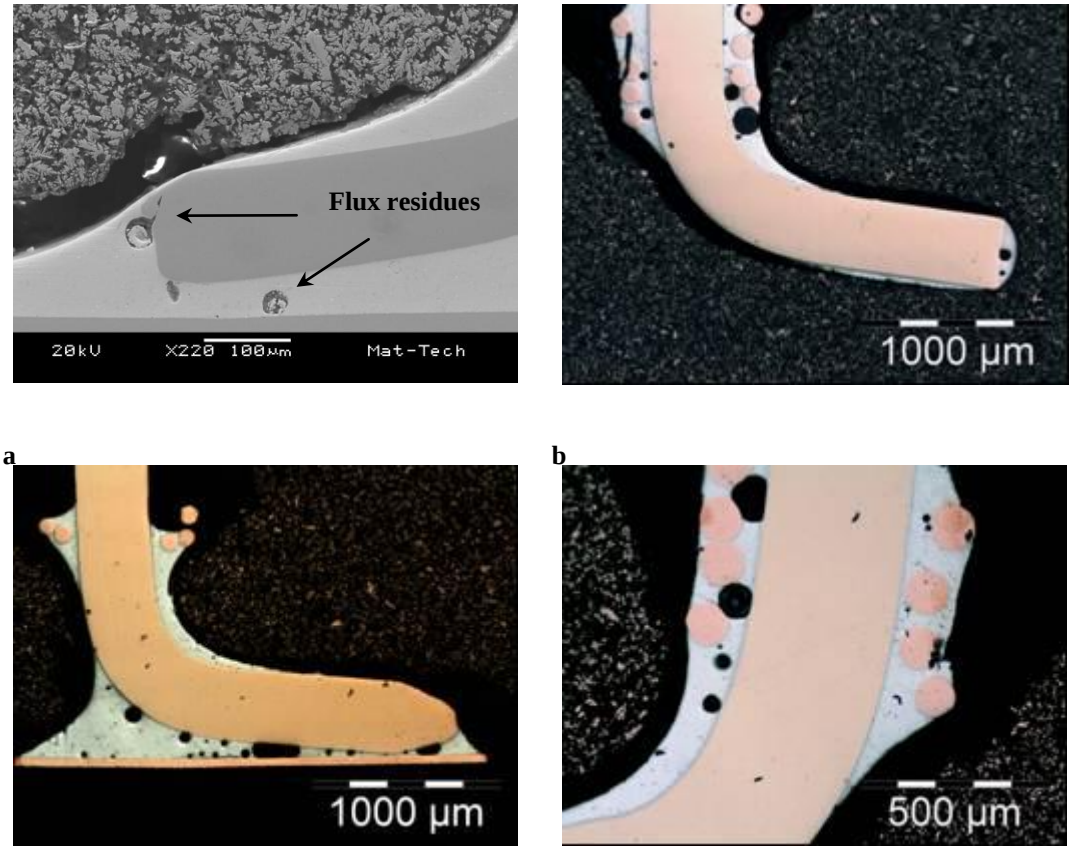

Figure 15 - (a) Secondary electron image and (b) (c) (d) optical image showing the cross section of different as-reflowed LF-components soldered using LF-paste: defects present in the as-reflowed samples.

3.6 LF-QFP and LF-paste: after accelerated thermal cycling test

The reliability of LF-components soldered with LF-paste in surface-mounted device components (SMD) with a Ni(P) finish has been investigated after thermo-cycle testing.

Due to the repeated thermal stresses and, in particular of the different expansion coefficient between the board and the LF-alloys, fractures are developed after thermal testing (Figures 16 and 17). Those images were collected from different samples having the identical composition and that were treated under the same thermal aging process. On the component shown is Figure 16, the highlighted crack is generated between the solder and the copper pad.

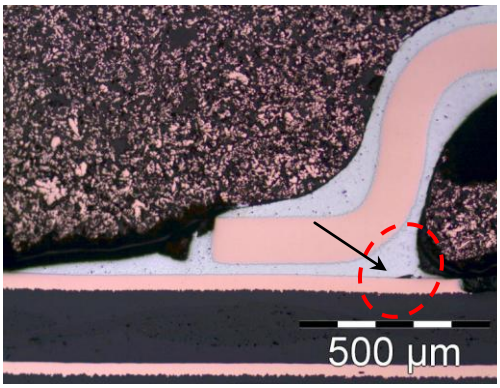

Figure 16 - Cross section of an LF-component soldered using LF-paste after accelerated thermal aging: fracture generated (optical microscope image).

In Figure 17, the enlargements of two fractures are illustrated. In both cases, crack initiation is found in the bulk solder, and it propagates perpendicularly to the joint surface.

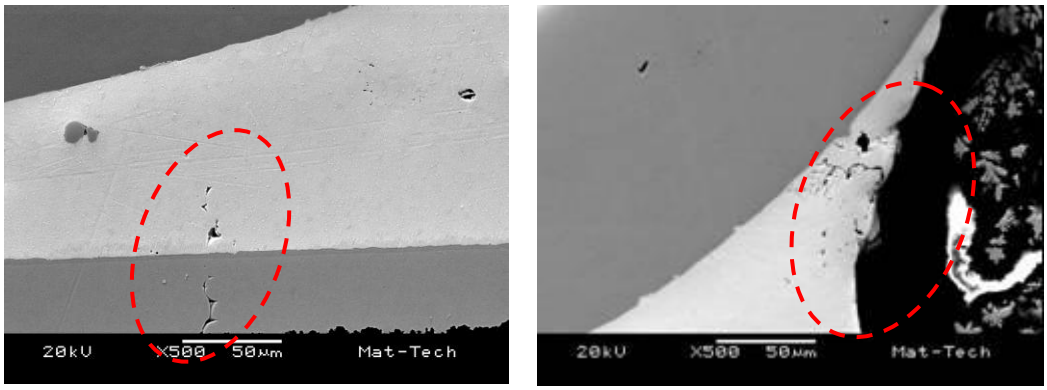

a **b**

Figure 17 - Cross section of a LF-component soldered using LF-paste after accelerated thermal aging: fracture generated (secondary electron image).

In addition, during the thermal tests the development of more (and bigger) voids together with the thermal induced stresses provokes the formation of wide fractures at the solder/joint interface as shown in Figure 18.

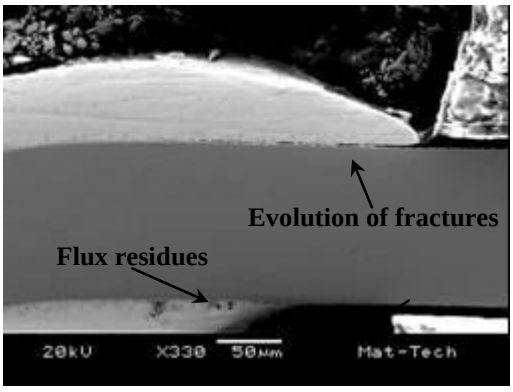

Figure 18 - Cross section of a LF-component soldered using LF-paste after accelerated thermal aging: fracture generated (secondary electron image).

The intermetallic layer on the thermally aged sample has an average thickness of 2.3-2.6 micrometers.

A portion of the intermetallic layer at the interface component/LF-paste after 1256 thermal cycles is shown in Figure 19. During reflow the Au layer is molten and the Ni has the ability to react with Sn and Cu forming intermetallics ($(Ni_xCu_y)_5Sn_6$). No intermetallics with gold were found.

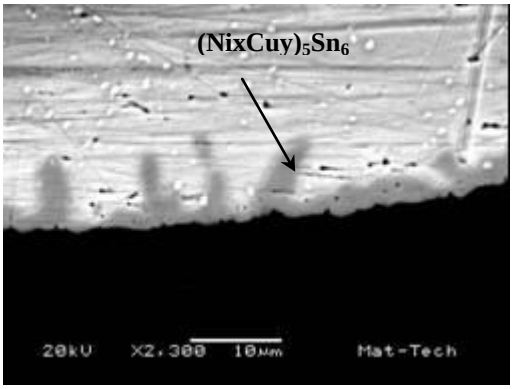

Figure 19 - Cross section of a LF-component soldered using LF-paste after accelerated thermal aging: intermetallic layer created at the component/LF-paste interface (secondary electron image).

The diffusion of the intermetallic compound stimulated by thermal aging increases the thickness of this phase in some areas (Figure 19). After reflow, Ag_3Sn was present all across the solder as spherical particles of dimensions lower than 1 micrometer. No Ag_3Sn platelets have been observed even on as-reflowed samples. The development of those particles is believed to be beneficial to the mechanical properties of the joint.

In Figure 20 is shown the intermetallic layer at the LF-paste/pad interface.

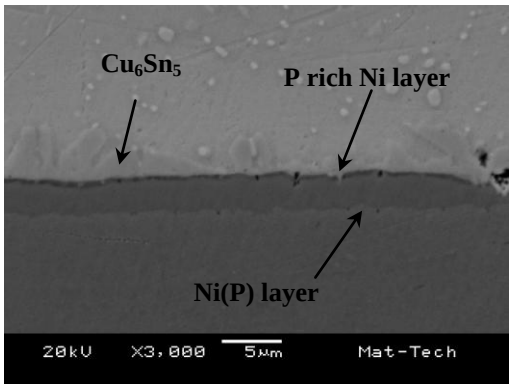

Figure 20 - Cross section of a LF-component soldered using LF-paste after thermal aging: intermetallic layer created at the LF-paste/pad interface (secondary electron image).

The composition of the intermetallic layer, that has scallop-like structure, is Cu_6Sn_5. According to EDX analysis, the composition of such intermetallic layer is of Cu-Ni-Sn. No evident presence of an intermetallic layer of Cu_3Sn was found below the Cu_6Sn_5 layer. The dark layer above the Ni(P) layer is attributed to the formation of a layer of enriched phosphorous due to the migration of Ni towards the solder. Voids were observed both at the LF-paste/Ni(P) and at the Ni(P)/Cu interfaces.

4 Conclusions

The microstructure of the IMC layer of different electronic components has been investigated for lead-containing and lead-free alloys. The following conclusions can be formulated:

A difference of peak temperature of ten degrees in the soldering process (225°C or 235°C) does not greatly influence the structure and thickness of the intermetallic layer in the lead-containing and lead-free solder systems that have been examined. In all cases, the segregation of lead at the interface solder/component, in lead-containing alloy joints, limits the growth of the intermetallic layer.

An ENIG finish might negatively affect the quality of a soldered joint. The formation of a phosphorous rich Ni layer at the interface solder/component facilitates the formation of a brittle layer and decreases the reliability of the joint.

Voids produced by the release of volatile species during the soldering process due to the application of no-clean flux were present. If compared with lead-containing alloy systems, lead-free alloy joints have larger and a higher amount of voids.

After accelerated thermal cycling tests on lead-free alloy systems, cracks and warpage of BGAs have been observed. Those defects were caused by the stresses generated during the soldering process due to the different expansion coefficients of the alloys in contact. In addition, the coalescence of the micrometric Kirkendall voids facilitates the development of fractures at the solder/component interface.

5 References

[1] Handbook of lead free solders technology for microelectronics assemblies edited by K. J. Puttlitz, K. A. Stalter.

[2] RoHS, Restriction of Hazardous Substances, S.I. 2006, No. 1463.

[3] Round robin testing and analysis of lead free solder pastes with alloys of tin, silver and copper - Final report. IPC solder products value council, 2005.

[4] K. Zeng, K. N. Tu, Mater. Sci. Eng. R 38 (2002) 55 - 105.

[5] D. Z. Li, C. Q. Liu, P. P. Conway, Materi. Sci. Eng. A: Struct. 391 (2005) 95 - 103.